Available online at www.sciencedirect.com
SCIENCE DIRECT®
Biochemical and Biophysical Research Communications 337 (2005) 313–319
BBRC
www.elsevier.com/locate/ybbrc

Constructing HIV-1 integrase tetramer and exploring influences of metal ions on forming integrase–DNA complex ☆

Li-Dong Wang, Chun-Li Liu, Wei-Zu Chen, Cun-Xin Wang *

College of Life Science and Bioengineering, Beijing University of Technology, Beijing 100022, China

Received 4 August 2005
Available online 19 September 2005

Abstract

HIV-1 integrase (IN) is essential for the replication of HIV-1 in human cells. At present, the complete structure of complex IN–DNA has not been resolved. In this paper, a HIV-1 IN tetramer model was built with homology modeling and molecular dynamics simulation approach, in which two Mg^{2+} ions were reasonably located in each catalytic core domain. Moreover, it was found that the AB and CD chains of HIV-1 IN tetramer were different in the structures and metal ions of HIV-1 IN tetramer might have great influences on DNA locating on IN. These findings may provide a more complete structural basis for guiding drug discovery and revealing integration mechanism.

Keywords: HIV-1 integrase; Molecular dynamics simulation; Metal ions

HIV-1 integrase (IN) is responsible for the integration of reversely transcribed viral DNA into host cell DNA. The full-length IN monomer is composed of one polypeptide chain which folds into three distinct functional domains: the N-terminal domain (NTD), the catalytic core domain (CCD), and the C-terminal domain (CTD). HIV-1 IN incorporates viral DNA into host chromosomal DNA through two metal-dependent step reactions [1–3,7].

However, there are still unresolved puzzles about the biochemical and biophysical mechanisms involved in these reactions. From experimental data, we can know that IN functions as an oligomer of the monomeric protein. What is the minimal IN molecule (tetramer, octamer or any other oligomer) to accomplish the concerted integration of both retroviral long terminal repeats still has different arguments in previous works [4,5]. At present, widely admitted results suggest that HIV-1 IN expressed in human cells is indeed present as a stable tetramer [4].

Several models of the HIV-1 IN–DNA complexes have been previously suggested [6,8,9,28]. A full-length HIV-1 IN dimer was built and, through an automated docking algorithm, the three-domain protein–viral DNA complex was gained [28]. An IN tetramer was formed by crystal lattice contacts bearing structural resemblance to a related bacterial transposase Tn5 [6]. Here, we propose an improved model that increases the precision of model in HIV-1 IN [4,10–14,25]. Crystallographic data of the IN catalytic domain reveal a single binding site for Mg^{2+}. However, many indirect proofs [11,12] suppose that HIV-1 IN may consist of two Mg^{2+} in its chains and has a reaction mechanism similar to those of other metal-dependent polymerases.

Furthermore, the linking parts of the NTD and CCD domains (residues 47–55) form a loop structure, which lead to determine the relative orientations of the NTD and the CCD difficultly. Moreover, reactions among atoms on the surface of the AB and CD chains may change the tetramer structure quite greatly against two lone dimers.

In this work, a whole IN tetramer was constructed; whose catalytic domain holds two Mg^{2+} ions. Furthermore, the flexibility of the loop structures and the influence

☆ *Abbreviations:* IN, integrase; NTD, N-terminal domain; CCD, catalytic core domain; CTD, C-terminal domain; MD, molecular dynamics; RMSD, root mean square deviation.

* Corresponding author. Fax: +86 10 67392837.
E-mail address: cxwang@bjut.edu.cn (C.-X. Wang).

0006-291X/$ - see front matter © 2005 Elsevier Inc. All rights reserved.
doi:10.1016/j.bbrc.2005.08.274

of atoms on the surface of AB and CD chains on the structure of whole tetramer were taken into account by using molecular dynamics simulation approach.

At last, by docking four different tetramers with B-form double DNA model, the influences of metal ions were considered quantificationally.

At present, scientists have not yet resolved the complete structure of complex IN–DNA, let alone the detailed mechanism about IN and DNA interactions. These findings may provide a more complete structural basis for guiding drug discovery and revealing integration mechanism.

Materials and methods

Model structure of the three-domain HIV-1 IN tetramer. The full-length HIV-1 IN tetramer was obtained by assembling the available domains in the Protein Data Bank (PDB). At first, a dimer was built [28]. The structure of catalytic core domain was built from chains A and B of the PDB structure 1QS4 [16] and 1BIS [17]. The position of first Mg^{2+} ion was consistent with that of Mg^{2+} ion of 1QS4. The second Mg^{2+} ion was placed in chains A and B in the same relative position according to PDB structure 1VSH [18]. The C-terminal domain of the dimer was later extracted by superimposing the CCD of PDB structure 1EX4 [19]. The N-terminal domains were finally added with the AB chains of PDB structure 1K6Y [6]. In the N-terminal domain, the lacking nine residues 47–55 were correctly placed by superimposing the 1WJD structure [21]. In order to gain a tetramer, the full-length dimer model was correctly superimposed with the 1K6Y structure.

Before docking the HIV-1 IN tetramer model with the viral DNA model, it was equilibrated through MD simulation with the program package GROMACS [22]. The simulation system was energy-minimized, using 2000 steps of the steepest descent method. Furthermore, the system was divided into two groups that tetramer was one group and others (SPC water and counter ions/CL−) was another. The whole system including solute and solvent was equilibrated for 1.2 ns at 300 K in the NTP ensemble. Periodic boundary conditions were used. A temperature coupling constant at 300 K was taken as 0.1 ps and a pressure coupling constant at reference pressure 1.0 bar was 0.5 ps.

In order to satisfy the need of docking program DOT [23], the average structure of MD equilibrium was modified taking advantage of AMBER8 [24]. After removing all the GROMACS' hydrogen in the model, polar hydrogen was added automatically. Furthermore, the model was relaxed by two-step energy minimizations which reduced the force constants from 500, 250 to 100 gradually. At the end, the final IN tetramer model structure was saved in pdb format.

Model structure of the viral DNA. The structure of 27 bp segment of viral DNA was built using the Biopolymer module of SYBYL [20], according to the following sequence: TAGTCAGTGTGGAAAATCTC-TAGCAGT/complement [26] in B-form. This structure was energy-minimized using 2000 steps of steepest descent.

Automated docking approach. In the present study, DOT program [23] was used as docking program. In the docking procession, simulation molecules were regarded as rigid body, and the intermolecular energy was calculated as a sum of electrostatic and van der Waals terms. Electrostatic potential file for the stationary molecule (IN) was prepared with the APBS program [27], in which the parameters were the following: the temperature of 300 K, the ionic strength of 150 mM, the solvent dielectric of 80, and the dielectric of 1 for the protein interiors. In the shape potential files of the stationary molecule (IN), the width of the van der Waals attractive layer equaled 0.3 nm. The shape of the moving molecule (DNA) was defined by its Cartesian coordinates of each atom and its charge distribution was represented by partial charges taken from the AMBER8 library. A rotation file with a set of 180,000 rotational orientations and a resolution of 2° was produced for the rotational search. For the translational search, the moving molecule was centered at each grid point (128^3 or about 2.1 million positions). Together, the rotational and translational search resulted in over 377 billion configurations ($128 \times 128 \times 128 \times 180{,}000 \approx 377.5$ billion) for the two molecules.

Results and discussion

Structure of the IN core domain

The catalytic domain of HIV-1 IN (residues 56–209) consists of the active site, which binds two Mg^{2+} ions required for catalysis [27,28]. The active site consists of two Asp and one Glu residues in the conserved D,D(35)E motif, each of which is required for catalysis [28,29]. In the present study, an IN tetramer was built with two Mg^{2+} in the corresponding chains core domains (Fig. 1). The relative position and distance of two Mg^{2+} ions were important in performing IN biological functions, because they might directly influence the surface potential of IN and the reciprocity of residues and metal ions, and even disturb proper DNA binding orientation. In this IN tetramer model, the distances of two Mg^{2+} ions in all four chains ranged from 0.390 to 0.531 nm, which were in accord with relative experimental data [11,12,15].

The structure of the HIV-1 IN tetramer

Some IN–DNA complexes were constructed in the previous works [6,9], but none of them had used an IN tetramer model that had undergone molecular dynamics (MD) simulation. In this paper, a well-founded tetramer model

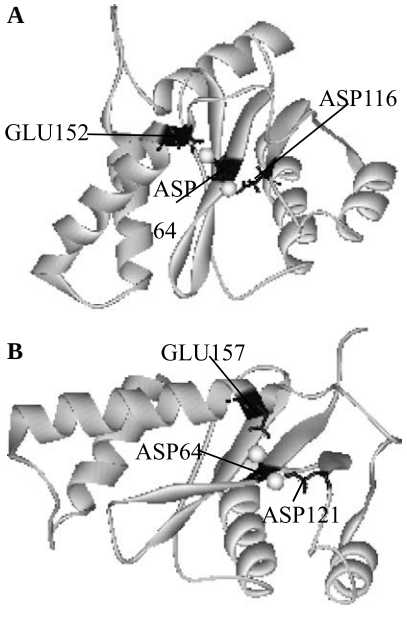

Fig. 1. Structures of the IN core domain. (A) The structure of the HIV-1 IN core domain. Residues ASP64, ASP116, and GLU152 are shown in ball-and-stick, and others are shown in ribbon diagram. Two Mg^{2+} ions are shown in balls. (B) The structure of the ASV IN core domain (PDB 1VSH). Residues ASP64, ASP121, and GLU157 are shown in ball-and-stick, and others are shown in ribbon diagram. Two Zn^{2+} ions are shown in balls.

was built before docking it with B-form DNA, and its information is shown in Figs. 2–4. From Fig. 2, we might see that, in the IN tetramer, there was no excess overlap and the metal ions located at the reasonable positions. Fig. 3 shows the root mean square deviation (RMSD) result of MD simulation. After 700 ps MD simulation, protein of IN tetramer reached equilibrium with tiny changes while Mg^{2+} ions reached equilibrium with a RMSD fluctuation less than 0.2 nm (0.2–0.4 nm). After 850 ps MD simulation, Zn^{2+} ions also reached equilibrium with unconspicuous movements (0.35–0.45 nm). Fig. 4 shows the total energy change of HIV-1 MD simulation system. After 700 ps MD simulation, the system was very stable.

Fig. 2. The tetramer of HIV-1 IN. Ribbon diagram of the tetramer from frontal view. A, B, C, and D chains are colored red, pink, blue, and green, respectively. Zn^{2+} ions are shown in green ball. Mg^{2+} ions are shown in yellow ball. (For interpretation of the references to color in this figure legend, the reader is referred to the web version of this paper.)

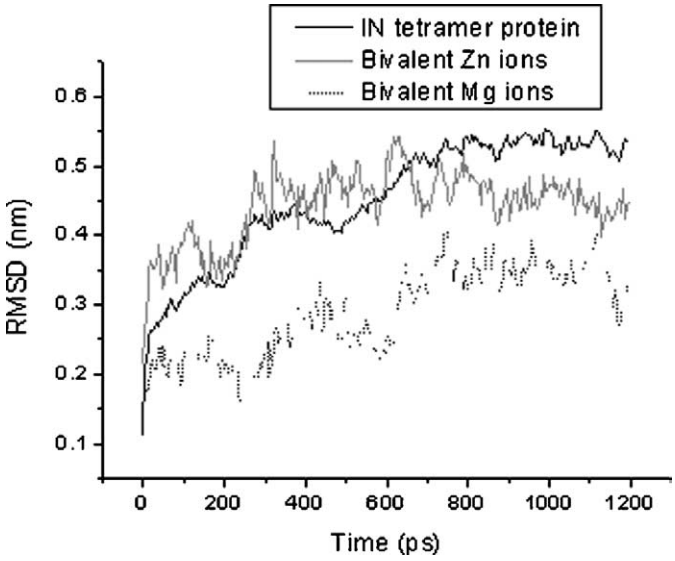

Fig. 3. The root mean square deviation (RMSD) of MD simulation HIV-1 IN tetramer relative to the structure of pre-MD simulation. The RMSD of IN tetramer' protein, Zn^{2+} ions, and Mg^{2+} ions are shown in different kinds of lines.

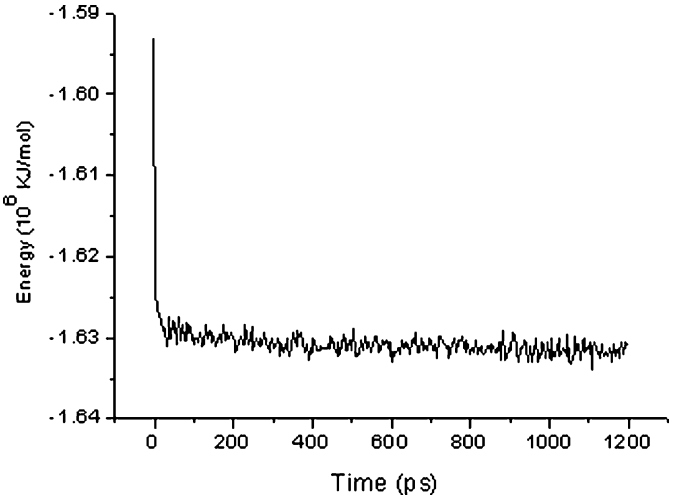

Fig. 4. The energy changes of MD simulation relative to the structure of pre-MD simulation. The total energy of the system is shown in black line.

In the previous works [6,9], AB and CD chains in the same HIV-1 IN tetramer had no differences due to their spatial symmetry. However, in Fig. 5, AB and CD chains' structural superimposition showed that they cannot be well superimposed in amino acid sequences because of their difference in spatial structure. The RMSD of all atoms for the AB chains and the CD chains was 3.644 nm. From Fig. 6, it was easy to find that the specific residues as well as the sum of residues involved in the interaction on the interface were very different. Especially, the amounts of hydrogen bonds and residues involving in hydrogen bonds were very different, which are shown in Fig. 6. Moreover, the characteristic of their hydrophilic and hydrophobic regions was marked by obvious distinction. For example, the hydrophobic regions of AB chains were obviously larger than the CD chains.

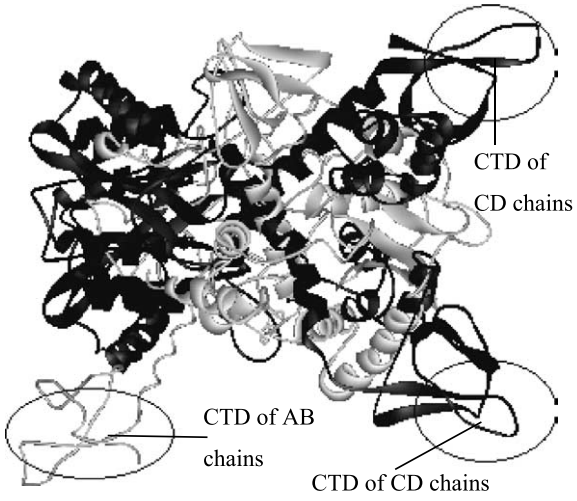

Fig. 5. The structural superimposed picture of AB and CD chains. The gray backbone and black backbone represent AB and CD chains, respectively. The image was created with insightII software [30].

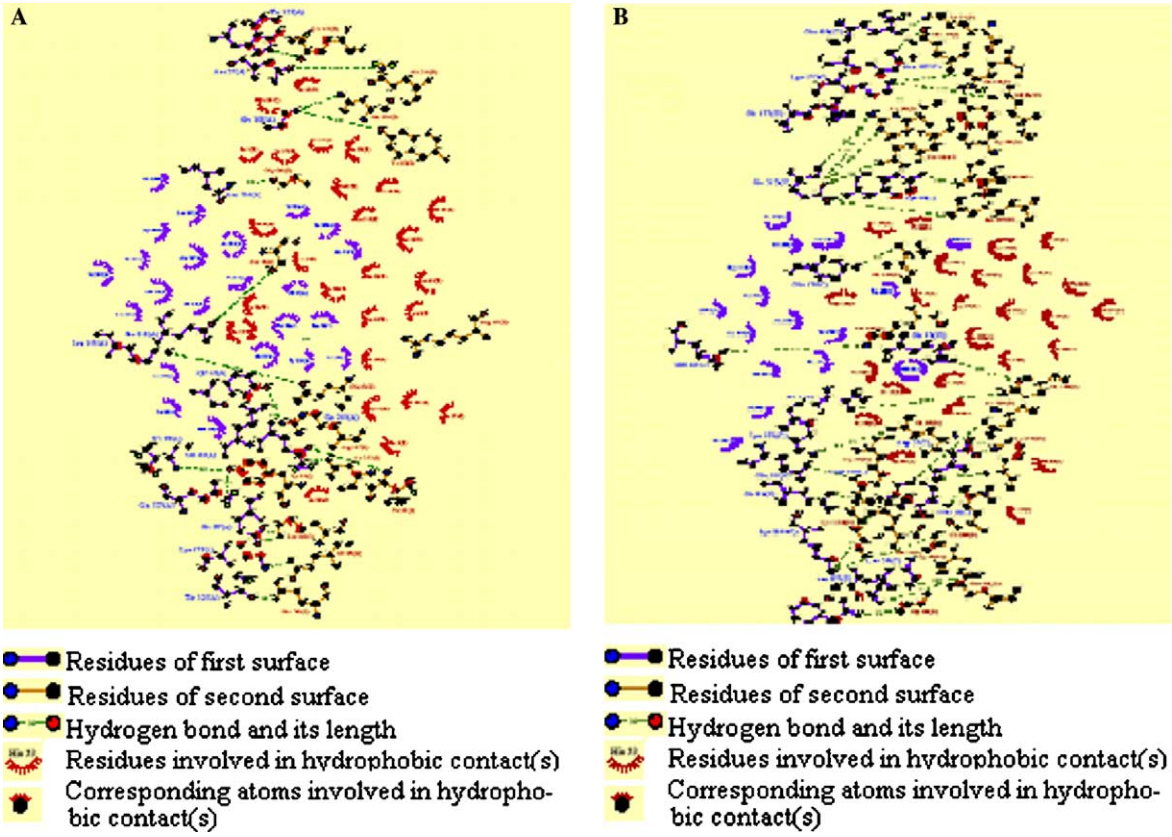

Fig. 6. The hydrophobic interaction of interface residues. (A) Hydrophobic interaction on the interface of AB chains. (B) For CD chains.

From that mentioned above, we suggest that, in the tetramer, the conformations of AB and CD chains are quite different, since in forming the tetramer, interactions did not just locate in the interior of the AB chains or the CD chains. In other words, the AB chains acting on the CD chains may sway configurations of all the chains and vice versa.

Docking results

It is still an issue about the influences of HIV-1 IN metal ions on IN–DNA binding modes. In this work, we docked DNA with four kinds of different IN tetramers, which comprised of no metal ions, one Zn^{2+}, one Zn^{2+} and one Mg^{2+}, and one Zn^{2+} and two Mg^{2+} ions in their chains, respectively. From the docking results, two different docking regions of IN tetramer tended very much to bind DNA. The two binding regions are shown in Fig. 7. Region 1 is the common regions above the CCD of A chain, the CCD of B chain, and the CTD of D chain. And region 2 is located in the mutual district above the CCD of C chain, the CTD of A chain, and the NTD of B chain. From previous works [14,31], we know that, when protein bonded DNA, electrostatic interactions are a major influencing factor. Electric potential distribution of the IN tetramer is shown in Fig. 8. Mg^{2+} ions located in the metal-binding site of three acidic residues (D,D(35)E), where vast nega-

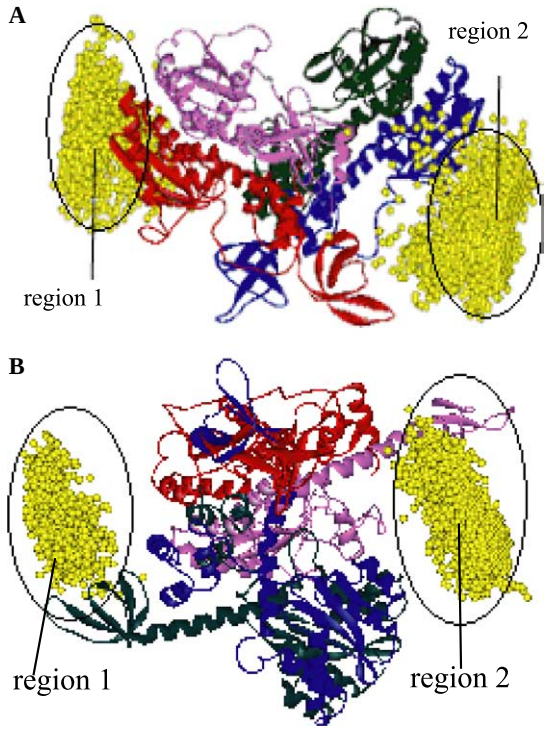

Fig. 7. Docking result of IN and DNA. (A) From frontal view, A, B, C, and D chains are colored red, pink, blue, and green, respectively. The geometric centers of DNA are shown in yellow balls. (B) The planform of HIV-1 IN tetramer. (For interpretation of the references to color in this figure legend, the reader is referred to the web version of this paper.)

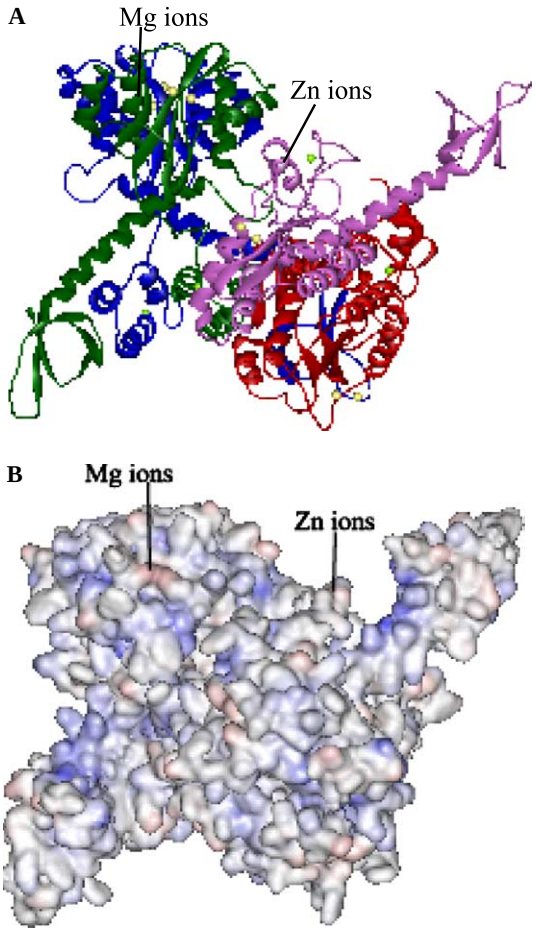

Fig. 8. The electric potential distribution of the HIV-1 IN tetramer. (A) The planform of HIV-1 IN tetramer. A, B, C, and D chains are colored red, pink, blue, and green, respectively. Zn^{2+} ions are shown in green ball. Mg^{2+} ions are shown in yellow balls. (B) Molecular surface of the IN tetramer in accord with the view shown in (A). Positive and negative electrostatic potentials are shown in blue and red. (For interpretation of the references to color in this figure legend, the reader is referred to the web version of this paper.)

tive charges were present. When Mg^{2+} ions formed bonds with these residues, electronegative nature of this region decreased greatly, which might make adjacent basic residues K156 and K159 easier to bond with phosphate of viral DNA.

From Table 1, total number of DNA fragments docking in region 2 increased gradually while that docking in region 1 decreased inchmeal consistent with metal ion numbers in the IN tetramer. When a Zn^{2+} ion was added to each chain, the numbers of DNA fragments in two regions changed greatly, from 9192 to 3740 in region 1 and 808 to 6260 in region 2. While the Mg^{2+} ions had also obvious effect on deoxyribonucleic acids locating on the IN surface. When one Mg^{2+} ion was added to the chains, the total number of docking DNA fragments in region 2 increased by about 500. After adding another Mg^{2+}, the total number in region 2 increased greatly again more than 1000.

Table 1
Comparison of the total numbers of DNA fragments in the two regions

Ion(s) in each chain	Total number	
	Region 1	Region 2
No metal ions	9192	808
1ZN	3740	6260
1ZN and 1MG	3255	6745
ZN and 2MG	2123	7877

In Fig. 9, four kinds of rectangles represent four different kinds of tetramer–DNA complexes. The altitude of each rectangle represents the number of IN–DNA complexes, and its width represents occupational energy scopes. In Fig. 9A, these rectangles were quite dispersive from −375 to −175 on *X*-axes. For each kind of rectangle, the altitude of the highest rectangle was not much larger than the second one, so neither of them was dominant in the corresponding total number. In other words, there were no dominant energy ranges for docking complexes of regions

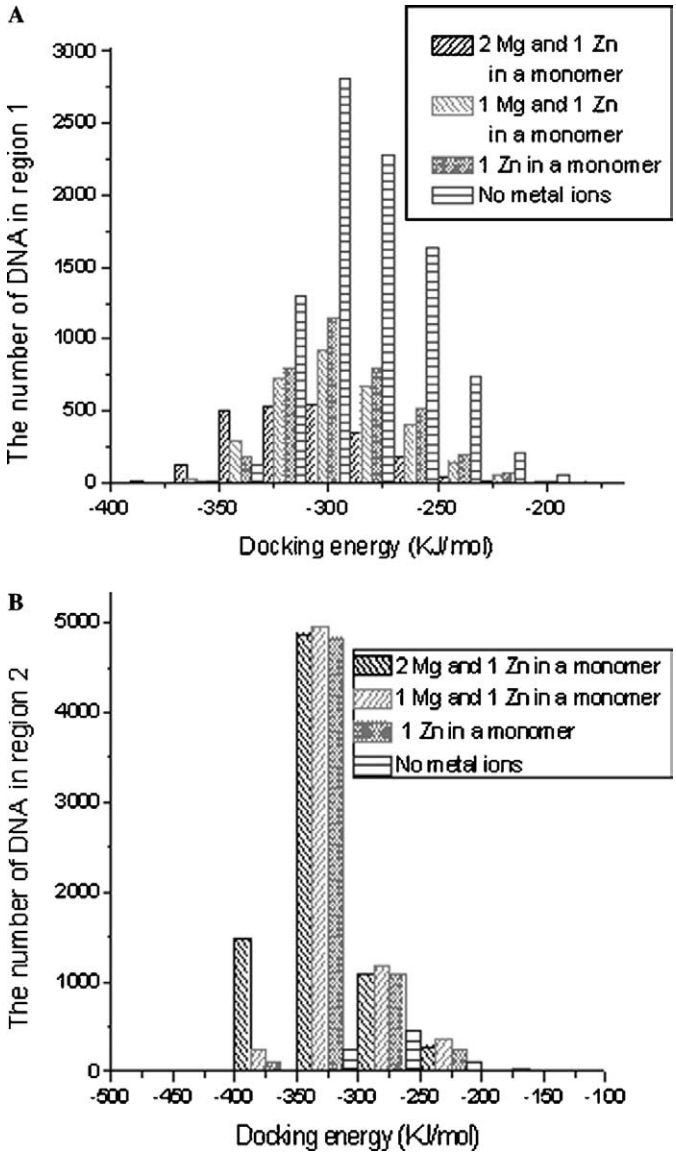

Fig. 9. Histogram of statistical graphs. (A) For docking complexes in region 1. (B) For docking complexes in region 2.

1. In Fig. 9B, for three kinds of rectangles with metal ions, each highest rectangle appeared near −330 on *X*-axes. It was worth noting that, the altitude of these rectangles was more than 4500 and even exceeded half of the respective total complex numbers. For tetramer without metal ions, the value of highest rectangle also exceeded half of its total complex number. In sum, there were remnant energy scopes in docking complexes of region 2.

We suppose that metal ions have different influences on docking results of two regions. After adding metal ions to the IN tetramer, IN–DNA complexes are prone to appear in region 2. And we hypothesize that both Mg^{2+} ions and Zn^{2+} ions have a great influence on DNA locating on IN.

Considering IN and DNA as rigid bodies, the present work finds the potential DNA-binding regions on IN and illustrates the effect of IN's metal ions on IN–DNA interaction. However, when long chain DNA binds with IN, its torsion and rotation make it possible to contact with multi-chains of IN synchronously. Here, using 27 bp B-form DNA we can consider this possibility to some degree. But this does not concern the flexibility of DNA. Furthermore, when IN and DNA form the complex, IN would effect further conformation changes [6,9,28].

The IN–DNA binding modes are complex and difficult to determine. Our ongoing work is to perform molecular dynamics simulation studies in order to gain the dynamics and conformation characteristics of the DNA–IN complex.

Acknowledgments

This work was supported in part by the Beijing Natural Science Foundation (Grant Nos. 5032002 and 5042003) and the Foundation from Beijing City Education Committee (Nos. KZ200410005002 and 20040005013).

References

[1] R.A. Katz, A.M. Skalka, The retroviral enzymes, Annu. Rev. Biochem. 63 (1994) 133–173.
[2] C.M. Farnet, F.D. Bushman, HIV cDNA integration: molecular biology and inhibitor development, AIDS 10 (1996) S3–S11.
[3] E. Asante-Appiah, A.M. Skalka, Molecular mechanisms in retrovirus DNA integration, Antiviral Res. 36 (1997) 139–156.
[4] P. Cherepanov, G. Maertens, P. Proost, B. Devreese, J.V. Beeumen, Y. Engelborghs, E.D. Clercq, Z. Debyser, HIV-1 integrase forms stable tetramers and associates with LEDGF/p75 protein in human cells, J. Biol. Chem. 278 (2003) 372–381.
[5] A.L. Faure, C. Calmels, C. Desjobert, M. Castroviejo, A. Caumont-Sarcos, L. Tarrago-Litvak, S. Litvak, V. Pariss, HIV-1 integrase crosslinked oligomers are active in vitro, Nucleic Acids Res. 33 (2005) 977–986.
[6] J.Y. Wang, H. Ling, W. Yang, R. Craigie, Structure of a two domain fragment of HIV-1 integrase: implications for domain organization in the intact protein, EMBO J. 20 (2001) 7333–7343.
[7] K.E. Yoder, F.D. Bushman, Repair of gaps in retroviral DNA integration intermediates, J. Virol. 74 (2000) 11192–11200.
[8] T.S. Heuer, P.O. Brown, Photo-cross-linking studies suggest a model for the architecture of an active human immunodeficiency virus type 1 integrase–DNA complex, Biochemistry 37 (1998) 6667–6678.
[9] A.A. Podtelezhnikov, J.A. McCammon, Modeling HIV-1 integrase complexes based on their hydrodynamic properties, Biopolymers 68 (2003) 110–120.
[10] S.P. Lee, J. Xiao, J.R. Knutson, M.S. Lewis, M.K. Han, Zn^{2+} promotes the self-association of human immunodeficiency virus type-1 integrase in vitro, Biochemistry 36 (1997) 173–180.
[11] C. Maurin, F. Bailly, E. Buisine, H. Vezin, G. Mbemba, J.F. Mouscadet, P. Cotelle, Spectroscopic studies of diketoacids–metal interactions. A probing tool for the pharmacophoric intermetallic distance in the HIV-1 integrase active site, J. Med. Chem. 47 (2004) 5583–5586.
[12] G. Bujacz, J. Alexandratos, A. Wlodawer, G. Merkel, M. Andrake, R.A. Katz, A.M. Skalka, Binding of different cations to the active site of avian sarcoma virus integrase and their effects on enzymatic activity, J. Biol. Chem. 272 (1997) 18161–18168.
[13] K. Pari, R.E. London, Solution structure of the RNase H domain of the HIV-1 reverse transcriptase in the presence of magnesium, Biochemistry 42 (2003) 639–650.
[14] A.A. Adesokan, J.M. Briggs, Prediction of HIV-1 integrase/viral DNA interactions in the catalytic domain by fast molecular docking, J. Med. Chem. 47 (2004) 821–828.
[15] J.F. Davies, Z. Hostomska, Z. Hostomsky, S.R. Jordan, D.A. Matthews, Crystal structure of the RNase H Domain of HIV-1 reverse transcriptase, Science 252 (1991) 88–95.
[16] Y. Goldgur, R. Craigie, G.H. Cohen, T. Fujiwara, T. Yoshinaga, T. Fujishita, H. Sugimoto, T. Endo, H. Murai, D.R. Davies, Structure of the HIV-1 integrase catalytic domain complexed with an inhibitor: a platform for antiviral drug design, Proc. Natl. Acad. Sci. USA 96 (1996) 13040–13043.
[17] Y. Goldgur, F. Dyda, A.B. Hickman, T.M. Jenkins, R. Craigie, D.R. Davies, Three new structures of the core domain of HIV-1 integrase: an active site that binds magnesium, Proc. Natl. Acad. Sci. USA 95 (1998) 9150–9154.
[18] G. Bujacz, M. Jaskolski, J. Alexandratos, A. Wlodawer, G. Merkel, R.A. Katz, A.M. Skalka, The catalytic domain of avian sarcoma virus integrase: conformation of the active-site residues in the presence of divalent cations, Structure 4 (1996) 89–96.
[19] J.C. Chen, J. Krucinski, L.J. Miercke, J.S. Finer-Moore, A.H. Tang, A.D. Leavitt, R.M. Stroud, Crystal structure of the HIV-1 integrase catalytic core and c-terminal domains: a model for viral DNA binding, Proc. Natl. Acad. Sci. USA 97 (2000) 8233–8238.
[20] SYBYL 6.5 Manual. Tripos Inc., 1699 South Hanley Rd, St. Louis, MO, USA, 1999.
[21] M. Cai, R. Zheng, M. Caffrey, R. Craigie, G.M. Clore, A.M. Gronenborn, Solution structure of the N-terminal zinc binding domain of HIV-1 integrase, Nat. Struct. Biol. 4 (1997) 567–577.
[22] D. Van der Spoel, A.R. van Buuren, E. Apol, P.J. Meulenhoff, D.P. Tieleman, A.L.T.M. Sijbers, B. Hess, K.A. Feenstra, E. Lindahl, R. van Drunen, H.J.C. Berendsen, Gromacs User Manual version 3.0, Nijenborgh 4, 9747 AG Groningen, The Netherlands. 2001, Internet: www.gromaccs.org.
[23] Y. Pommier, A.A. Pilon, K. Bajaj, A. Mazunder, N. Neamati, DOT User's Guide, version 1.0 Beta, The Computational Center for Macromolecular Structures, San Diego Supercomputer Center: San Diego, CA, 1998.
[24] D.A. Case, T.A. Darden, T.E. Cheatham III, C.L. Simmerling, J. Wang, R.E. Duke, R. Luo, K.M. Merz, B. Wang, D.A. Pearlman, M. Crowley, S. Brozell, V. Tsui, H. Gohlke, J. Mongan, V. Hornak, G. Cui, P. Beroza, C. Schafmeister, J.W. Galdwell, W.S. Ross, P.A. Kollman, AMBER 8, University of California, San Francisco, 2004.
[25] A.S. Espeseth, P. Felock, A. Wolfe, M. Witmer, J. Grobler, N. Anthony, M. Egbertson, J.Y. Melamed, S. Young, T. Hamill, J.L. Cole, D.J. Hazuda, HIV-1 integrase inhibitors that compete with the target DNA substrate define a unique strand transfer conformation for integrase, Proc. Natl. Acad. Sci. USA 97 (2000) 11244–11249.
[26] N.A. Baker, D. Sept, S. Joseph, M.J. Holst, J.A. McCammon, Electrostatics of nanosystems: application to microtubules and the ribosome, Proc. Natl. Acad. Sci. USA 98 (2001) 10037–10041.

[27] M.D. Andrake, A.M. Skalka, Retroviral integrase, putting the pieces together, J. Biol. Chem. 271 (1996) 19633–19636.
[28] L.D. Luca, A. Pedretti, G. Vistoli, M.L. Barreca, L. Villa, P. Monforte, A. Chimirri, Analysis of the full-length integrase–DNA complex by a modified approach for DNA docking, Biochem. Biophys. Res. Commun. 310 (2003) 1083–1088.
[29] A. Engelman, R. Cragie, Identification of amino acid residues critical for human immunodeficiency virus type 1 protein in vitro, J. Virol. 66 (1992) 6361–6369.
[30] InsightII, Accelrys, Inc., San Diego, CA, http://www.accelrys.
[31] Y.F. Deng, J. Glimm, Y. Wang, A. Korobka, M. Eisenberg, A.P. Grollman, Prediction of protein binding to DNA in the presence of water-mediated hydrogen bonds, J. Mol. Model. 5 (1999).